Polarization analysis of speckle field below its transverse correlation width : application to surface and bulk scattering

Jan Dupont,[1] Xavier Orlik,[1,*] A. Ghabbach,[2] M. Zerrad,[2] G. Soriano,[2] and C. Amra[2]

[1]*ONERA, Theoretical and Applied Optics Department, 31055 Toulouse, France*
[2]*Institut Fresnel CNRS, Universités d'Aix-Marseille, Ecole Centrale Marseille, Domaine Universitaire de Saint-Jérôme, 13397 Marseille Cedex 20, France*

[*]*xavier.orlik@onera.fr*

Abstract: An experimental method for accurate polarimetric characterization of speckle field below its transverse correlation width is proposed. Using a polarimetric analyzer, the speckle field under investigation is probed by a set of polarimetric projections describing the full Poincaré sphere surface. Spatial polarimetric variations of the speckle field are thus observed with an accuracy of 1% for each Stokes parameter. Moreover, all the experimental data can be guaranteed by a validity criterion. Using white paper sheet and rough metal samples, the method exhibits strong potential to analyze and differentiate speckle fields generated by bulk and surface scattering.

OCIS codes: (120.5410) Polarimetry; (030.6140) Speckle; (260.5430) Polarization; (110.5405) Polarimetric imaging; (110.6150) Speckle imaging.

References and links

1. J. W. Goodman, *Speckle Phenomena in Optics* (Roberts & Company Pub., 2007) 48-50.
2. I. Bergoënd, X. Orlik, and E. Lacot, "Study of a circular Gaussian transition in an optical speckle field," J. Europ. Opt. Soc. **3**, 1990–2573 (2008).
3. O. Vasseur, I. Bergoënd, and X. Orlik, "A Gaussian transition of an optical speckle field studied by the minimal spanning tree method," J. Europ. Opt. Soc. **5**, 10052 (2010).
4. P. Bergström, D. Khodadad, E. Hällstig, and M. Sjödahl "Dual-wavelength digital holography: single-shot shape evaluation using speckle displacements and regularization," Appl. Opt. **53**, 123–131 (2014).
5. J. Petit, G. Montayb, and M. François "Strain rate measurements by speckle interferometry for necking investigation in stainless steel," Int. J. Solids Struc. **51**, 540–550 (2014).
6. L. Tchvialeva, G. Dhadwal H. Lui, S. Kalia, H. Zeng, DI. McLean, and TL. Lee, "Polarization speckle imaging as a potential technique for in vivo skin cancer detection," J. Biomed. Opt. **6**, 061211 (2013).
7. M. Zerrad, J. Sorrentini, G. Soriano, and C. Amra, "Multiscale spatial depolarization of light," Proc. SPIE 8171, Physical Optics, 81710C (2011)
8. L. Pouget, J. Fade, C. Hamel, and M. Alouini, "Polarimetric imaging beyond the speckle grain size," Appl. Opt. **51**, 7345–7356 (2012).
9. A. Ghabbach, M. Zerrad, G. Soriano, and C. Amra, "Accurate metrology of polarization curves measured at the speckle size of visible light scattering," Opt. Express **22**(12), 14594–14609 (2014).
10. G. G. Stokes, Trans. Camb. Phil. Soc., **9**, 399 (1852).
11. D. H. Goldstein, *Polarized Light* (CRC Press, 2003) 34.
12. H. Poincaré, *Théorie mathématique de la lumière* (GABAY, 1892).

#218866 - $15.00 USD Received 28 Jul 2014; revised 29 Aug 2014; accepted 29 Aug 2014; published 25 Sep 2014

13. J. Sorrentini, M. Zerrad, and C. Amra, "Statistical signatures of random media and their correlation to polarization properties," Opt. Lett. **34**, 2429–2431 (2009).
14. G. Soriano, M. Zerrad, and C. Amra, "Enpolarization and depolarization of light scattered from chromatic complex media," Opt. Express **22**, 12603–12613 (2014).

1. Introduction

When a coherent beam either illuminates a surface rough on the scale of the wavelength or crosses a medium that provokes random spatial dephasing of the field, the multitude of dephased contributions generate along propagation in space, interference effects. The resulting field that exhibits fast spatial variations of intensity is called speckle. An extremely dense literature is available on the subject because speckle is omnipresent in optics, radar and ultrasound applications. In some cases, speckle represents a noise to reduce. Several methods can be used as temporal averaging with a moving diffuser, polarization diversity, wavelength and angle diversity, temporal and spatial coherence reduction [1]. In other applications, the study of the speckle on the contrary brings interesting data about the surface or the medium responsible of these interferences. Especially, it has been shown that a variable illumination spot size could describe the transition from non Gaussian to Gaussian statistics of a speckle field generated by a rough surface and could bring usefull information about its roughness characteristics [2, 3]. Other applications such as deformation and strain field analysis, digital holography [4], and speckle interferometry [5] can be cited. Recently, in the biomedical field, in vivo skin cancer detection by polarization speckle imaging has shown some promising results [6]. In spite of the numerous applications of speckle fields, our knowledge about how are spatially structured their State Of Polarization (SOP) and their associated Degree Of Polarization (*DOP*) remain until now very limited. Such knowledge implies to perform several acquisitions of intensity in various optical configurations but a speckle field, as an interference phenomenon, is extremely sensitive to any phase variation during the acquisition procedure. Thus to perform such study on a scale below the transverse correlation width of the speckle field is very challenging and the polarimetric accuracy of the procedure has to be checked carefully. Until now, only a few works have tried such characterization [7–9]. We provide in this work an new experimental method to map very accurately the SOP and the associated *DOP* of a speckle field at a scale below its transverse correlation width, with a criterion ensuring the accuracy and validity of the experimental results. Application to polarimetric analysis of speckle fields generated by surface and bulk scattering is proposed.

2. Polarimetric Analysis by Full Projection in the Poincaré Space

A classical method to determine the polarization state of a field, eventually partially polarized, consists in the acquisition of the 4 Stokes parameters [10] : S_0 represents the total intensity of the light, S_1 the amount of linear horizontal minus the amount of vertical polarized light, S_2 the amount of linear +45 ° minus the amount of -45 ° polarized light, and S_3 the amount of left circular minus the amount of right circular polarized light [11]. The Degree Of Polarization (*DOP*) of the field is then defined by :

$$DOP = \frac{\sqrt{S_1^2 + S_2^2 + S_3^2}}{S_0}$$

A *DOP* equal to 1 represents a totally polarized light whereas a value lower than 1 represents a partially polarized light.
Except for the first component S_0, the 3 other components need subtraction of experimental data to be determined. Using an imaging system with a charged coupled device (CCD) camera, this

#218866 - $15.00 USD Received 28 Jul 2014; revised 29 Aug 2014; accepted 29 Aug 2014; published 25 Sep 2014

constraint can become severe in terms of polarimetric accuracy because of the non linearity of the CCD camera and eventual mechanical movements during the switch between polarimetric states of analysis. Care has to be taken also to the wavefront variation of the field during the full acquisition procedure of the polarimetric structure of the speckle field [8]. Moreover, even in case the setup allows to switch between different polarimetric states of analysis without any mechanical movement, for example using Nematic Liquid Crystals (NLC), a non perfect perpendicular incidence between the beam and the NLC can cause a non constant deviation of the beam in function of the requested birefringence. As a consequence, our first tries to map accurately the polarization of speckle fields failed by giving some polarimetric states with a *DOP* clearly higher than 1, thus showing an extremely low experimental accuracy. We notice that in [8], even a careful protocol involving a constant wavefront during acquisition of the SOP of the speckle field gave rise to some numerous pixels with *DOP* reaching near 1.5. Due mainly to the reasons cited above that prevent among us, high polarimetric accuracy, we have elaborated the State Of Polarization Analysis by Full Projection in the Poincaré space method (SOPAFP) that avoids any subtraction of intensity and moreover checks the validity of the obtained SOP.

This method uses a Polarimetric State Analyzer (PSA) which consists of 2 variable birefringent materials (2 NLC called CL3 and CL4) with eigen axes oriented respectively at 45° from each other, followed by a quarter waveplate and a linear vertical polarizer with eigen axes respectively oriented at 45° from each other. The 2 orientation constraints cited above between the 2 nematic liquid crystals CL3 and CL4 and between the quarter waveplate and the linear polarizer ensure that the PSA can project an incident field on any fully polarized polarimetric state of the Poincaré Sphere [12].

We define a projection state of our PSA as follow : the variable birefringences δ_3 and δ_4 of respectively CL3 and CL4 for a given polarimetric state of projection *i* are chosen so that if the polarimetric state *i* is effectively incident on the PSA, it will exit after CL3, CL4 and the quarter waveplate, with a vertical linear polarization perfectly aligned with the output linear polarizer, thus giving rise to a maximum transmitted intensity. All other polarimetric incident states but *i* will be partially absorbed excepted the state diametrically opposed to *i* on the Poincaré sphere that will be completely absorbed (in case of a perfect linear polarizer).

In order to perform the various polarimetric projections of the speckle field to analyze, the Poincaré sphere surface is uniformly discretized into projection states. For a polarimetric accuracy of 1%, 300 projection states were needed. As an illustration, the Fig. 1(a) shows the first projections states that are used for polarimetric speckle analysis. We have chosen arbitrarily to scan from the initial state $(1;0;-1;0)$ to the final one $(1;0;1;0)$. For a given electromagnetic field to analyze, the full discretized surface of the Poincaré sphere is scanned. As an illustration, the Fig. 1(b) shows the theoretical variation of intensity transmitted through the PSA in the hypothesis of an incident electromagnetic field of state $(1,-0.58,-0.58,-0.58)$ represented by a green circle in Fig. 1(a).

#218866 - $15.00 USD Received 28 Jul 2014; revised 29 Aug 2014; accepted 29 Aug 2014; published 25 Sep 2014

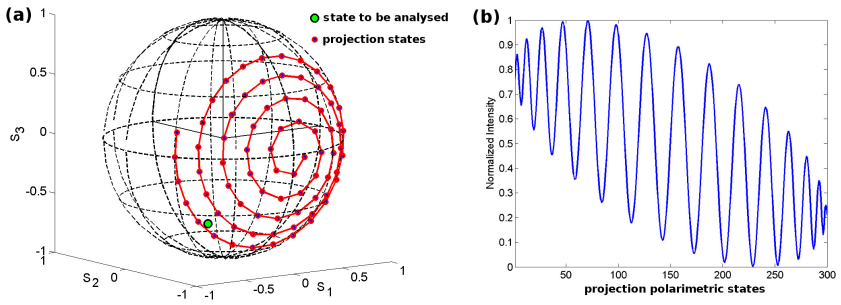

Fig. 1. (a) First polarimetric states of projection homogeneously distributed at the surface of the Poincaré sphere. During the acquisition procedure used for polarimetric analysis, the incident field is projected sequentially on every projection state by the use of the PSA. The green disc corresponds to the SOP of the field that is being analyzed. (b) Simulated variation of intensity at the output of the PSA and corresponding to the projections of the incident field shown in (a). Each curve of intensity variation during such a scan signs a unique incident SOP.

To each polarimetric state of the incident field corresponds a unique variation of intensity during the scan over the projection states. During this scan, the projection state that is the closest to the polarimetric state of the incident field will give rise to maximum intensity at the output of the PSA. On the contrary, when the incident state of illumination is projected on the more diametrically opposed state, the output will be minimum. As a consequence, just by recording the projection states associated to the minimum and maximum of intensity transmitted through the PSA during the scan, we obtain the polarimetric illumination state with its associated *DOP*. However, to increase our accuracy and to allow the obtained polarimetric states to be everywhere on the Poincaré sphere and not only on the discretized projection states, we fit the complete experimental curve of the intensity variation with a theoretical one using the 4 Stokes parameters S_0, S_1, S_2, S_3 as adjustable variables for the polarimetric incident state. Thus, we use the whole ensemble of experimental polarimetric projections for maximum accuracy and each experimental polarimetric state is obtained with a characteristic distance that quantifies the difference between the closest possible theoretical variation of intensity and the experimental one. This distance is used to filter physical states from nonphysical ones and provide us a criterion of validity of the obtained SOP. Non physical results could come mainly from the non linearity of the CCD camera especially in low intensity places of destructive interferences, from the wavefront variation and/or from the deviation of the beam, during acquisition procedure. The experimental setup is shown on Fig. 2.

#218866 - $15.00 USD Received 28 Jul 2014; revised 29 Aug 2014; accepted 29 Aug 2014; published 25 Sep 2014

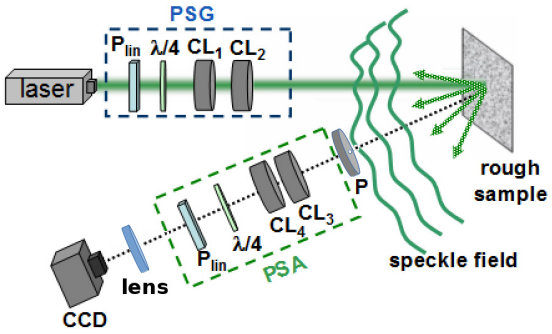

Fig. 2. Scheme of the experimental setup. A laser diode emits a beam at 532 nm through the Polarization State Generator (PSG) composed of a linear vertical polarizer P_{lin} and a quarter waveplate $\lambda/4$ oriented at 45 ° from each other, followed by 2 nematic liquid crystals LC_1 and LC_2 with their eigen axis oriented at 45 ° from each other. The quarter waveplate of the PSG ensures the ability to generate any Stokes vector on the Poincaré sphere surface, whatever the orientation of the entrance linear polarizer is. After scattering on the sample, the field goes through a pinhole P before entering the PSA that is composed of the same optical elements than the PSG but in reverse order. Its quarter waveplate is not essential but makes our calibration procedure easier by keeping the symmetry between the PSG and the PSA.

The pinhole at the entrance of the PSA is used to choose the transverse correlation width of the speckle field with respect to the pixel size and imaging optics. Some Polarimetric State Generator (PSG) and Analyzer (PSA) enable us respectively to generate the illumination field and to project the field scattered by the sample using any polarization state chosen at the surface of the Poincaré sphere.

After a first calibration procedure of our 4 nematic liquid crystals, a second procedure checks and refines automatically the voltages corresponding to each projection state of the PSA using a TPX Polarimeter from Thorlabs[(c)] as a reference. We reach finally a polarimetric accuracy of 1% in the 3 Stokes parameters S_1, S_2, S_3 of all the 300 polarimetric projection states. Several tests using different polarimetric states of illumination on a mirror have then confirmed that this accuracy is conserved for the polarimetric states detected by the SOPAFP method. Moreover, such test experiments have allowed to define a threshold value as a criterion for which the experimental variation of intensity during an acquisition procedure is close enough to theory to consider the polarization state determined by the SOPAFP method as valid. This threshold value is characteristic of our experiment and is used in the forthcoming sections to ensure the same accuracy of 1% for every polarization state detected from the speckle fields. The experimental variations of intensity that do not respect this threshold value are removed before processing the statistics of the speckle field.

3. Comparison of classical and SOPAFP methods for Stokes vector analysis

We generate in this section a speckle field by the scattering from a rough metallic surface at the wavelength 532 nm. Using exactly the same optics and the same part of speckle field to analyze, we perform the experimental acquisition using the classical method (images subtraction) to extract the Stokes parameters and the SOPAFP method described above. We show in Fig. 3 the spatial representation of the SOP of the field using RGB representation where $R = \mid S_1 \mid$, $G = \mid S_2 \mid$, $B = \mid S_3 \mid$. Figure 3(a) corresponds to the classical method and Fig. 3(b) to the SOPAFP method. Figure 3(c) shows the corresponding *DOP* histogams.

#218866 - $15.00 USD Received 28 Jul 2014; revised 29 Aug 2014; accepted 29 Aug 2014; published 25 Sep 2014

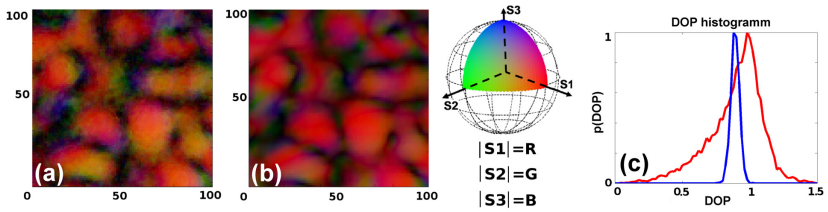

Fig. 3. Representation of the spatial variations of the SOP of a speckle field generated by a rough metallic surface and analyzed in terms of Stokes parameters using (a) subtraction of intensity images and (b) the SOPAFP method. In this RGB color representation, $R = \mid S_1 \mid$, $G = \mid S_2 \mid$, $B = \mid S_3 \mid$ where the values of R, G and B vary from 0 to 1. (c) *DOP* histograms : the red curve corresponds to the classical method and the blue one to the SOPAFP method.

We notice that this RGB color representation doesn't take into account the sign of the Stokes parameters but allows an interesting overview of the spatial variation of the states of polarization. In the case of the determination of Stokes parameters using images subtraction, in addition to the noisy signal that can be observed in Fig. 3(a), the corresponding red histogram in Fig. 3(c) exhibits a *DOP* mean value of 0.90 with a large standard deviation of 0.2 and numerous values higher than 1, thus nonphysical. The SOPAFP method shows in Fig. 3(b) a less noisy signal in the RGB color representation, and its *DOP* histogram exhibits the mean value of 0.90 but with a much smaller standard deviation of 0.03 without any value higher than 1.

4. Application to speckle fields generated by surface and bulk scattering

From the theoretical point of view, we know that the histogram statistics of intensity of speckle fields generated by surface and bulk scattering, in most situations, can be differentiated by their gamma laws of different orders [13]. To go further in the statistical analysis, we propose now a comparative analysis of speckle fields generated by scattering from a rough metallic surface of aluminium and from a white sheet of paper in order to compare the spatial variations of the SOP of speckle fields generated by surface and bulk scattering. Figs. 4(a) and 4(e) show respectively for the rough metal surface and the white sheet of paper, the sum of all the intensity images obtained by projection of the speckle field over the 300 projection states used in the SOPAFP method. During the acquisition procedure, the speckle field generated by surface scattering has exhibited a near constant pattern with a global variation of intensity depending of the projection state. On the contrary, the speckle field generated by bulk scattering has exhibited very different intensity patterns in function of the projection states. Figs. 4(b) and 4(f) show the corresponding spatial variations of the *DOP*. The criterion of validity described in the previous section has been used to check which pixel of the CCD camera, during the acquisition procedure, has exhibited an acceptable variation of intensity ensuring an accuracy of 1% in each Stokes parameter of the SOP. The resulting areas of acceptable pixels has been encircled by dotted lines and we observe that they remove pixels with too low intensity that correspond to places of strong destructive interferences. Figs. 4(c) and 4(g) represent the corresponding variations of the SOP represented in RGB color. In order to visualize how vary the SOP in function of the origin of the scattering (surface or bulk), Figs. 4(d) and 4(h) show some trajectories of the SOP in the Poincaré space corresponding to the full vertical cross sections at the middle of respectively Figs. 4(c) and 4(g). We observe that the SOP remains localized in the case of surface scattering while it spreads apparently randomly in the Poincaré sphere in the case of bulk scattering. An additional but smaller cross section named (A) in Fig. 4(g) has been plotted in Fig. 4(h) in order to better quantify the corresponding length traveled by the SOP.

#218866 - $15.00 USD Received 28 Jul 2014; revised 29 Aug 2014; accepted 29 Aug 2014; published 25 Sep 2014

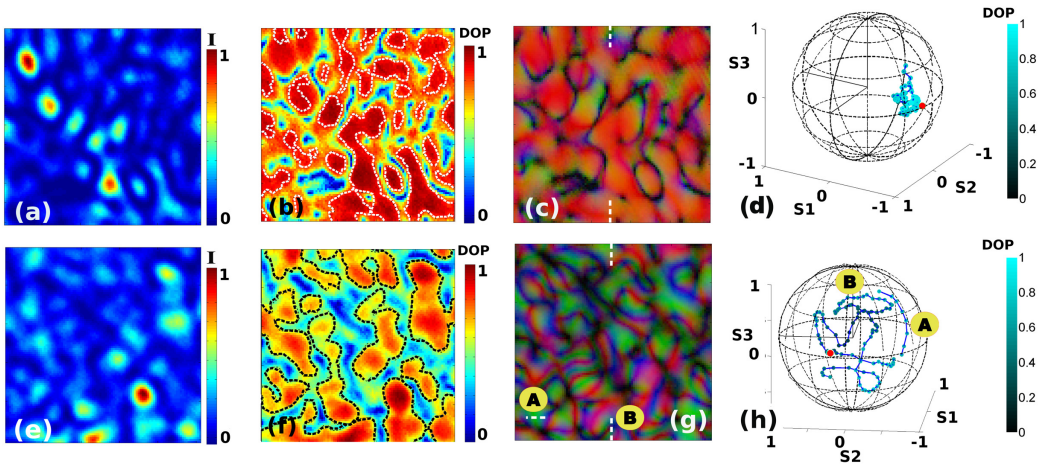

Fig. 4. For respectively the scattering from a rough metal (upper line) and from a white paper sheet (lower line) : (a) and (e) show the sum of intensity images obtained by the whole set of polarimetric projections, (b) and (f) the degree of polarization with filtered physical results that are encircled by dotted lines, (c) and (g) the RGB representation of polarimetric states, (d) and (h) the Poincaré sphere representation of the full vertical cross section of the middle of respectively figure (c) and (g) as indicated by white dotted lines. The red dots represent the initial states of illumination. An additional cross section analysis named A in (g) is plotted on (h). Polarimetric states remain localized with high *DOP* values in the case of surface scattering while they spread all over and inside the Poincaré sphere with lower *DOP* values in the case of bulk scattering.

Then, the areas of pixels selected by the validity criterion [Figs. 4(b) and 4(f)] have been analyzed deeper from the point of view of statistics in Fig. 5. Figures 5(a) 5(c) 5(e) show the *DOP* histograms of the fields for respectively a mirror, a rough metal surface and a white sheet of paper as sample. Figs. 5(b) 5(d) 5(f) show the corresponding SOP in the Poincaré sphere. The mirror has been used as a reference sample to test the point spread function of the SOPAFP method and moreover to define the corresponding threshold value for the validity criterion as explained in the previous section. The *DOP* mean values are found to be respectively 0.97 with a standard deviation of 0.01 for the mirror, 0.88 with a standard deviation of 0.04 for the rough metal surface, and 0.64 with a standard deviation of 0.11 for the white paper sheet. We can observe clearly that the SOP of the speckle field originating from surface scattering remains very localized and near the surface of the Poincaré sphere, keeping the information about the illumination polarization state while the speckle field originating from bulk scattering spreads near all over the sphere.

#218866 - $15.00 USD Received 28 Jul 2014; revised 29 Aug 2014; accepted 29 Aug 2014; published 25 Sep 2014

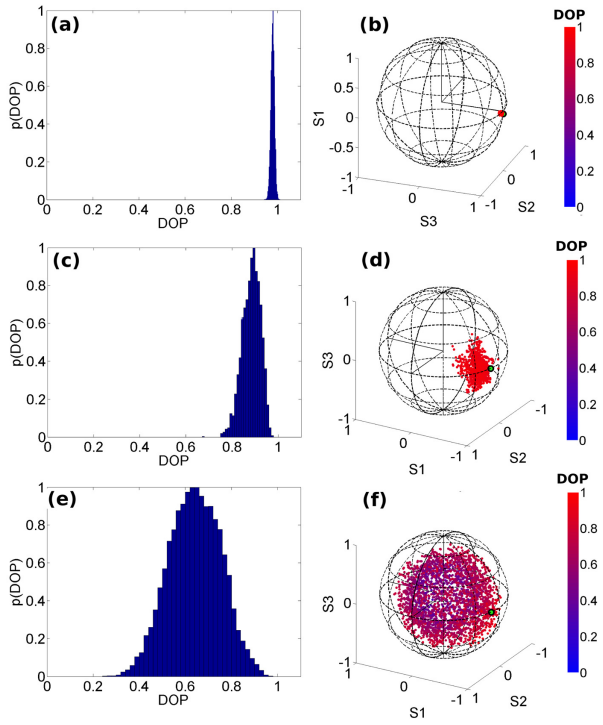

Fig. 5. (a) (c) (e) show the *DOP* histograms of the fields scattered from respectively a mirror, a rough metal sample and a white paper sheet. (b) (d) (f) show the corresponding Poincaré sphere representation of the SOP. The green dots represent the illumination polarimetric states.

5. Conclusion

We have proposed a new method to study with high accuracy the polarimetric properties of speckle fields at a scale below their transverse correlation width. By using a polarimetric analyzer allowing polarimetric projections homogeneously distributed on the full Poincaré sphere surface, an accuracy of 1% in each Stokes parameter of the analyzed speckle field has been obtained. Comparison with classical setup devoted to Stokes analysis that uses simple image subtractions has been proposed. The new method has been applied to analyze speckle fields coming from surface and bulk scattering. The spatial variations of the polarimetric states and the associated degree of polarization have been studied in both cases. The speckle field generated by surface scattering using a rough metal sample mainly maintains the polarimetric state of the illumination and exhibits only a small polarimetric spread near the surface of the Poincaré sphere, thus keeping a high *DOP* of mean value around 0,88 with a standard deviation of 0.04. The speckle field generated by bulk scattering using a white sheet of paper exhibits on the contrary, due to multiple scattering, a very strong spreading of the polarimetric states all over the Poincaré sphere with an associated mean *DOP* value around 0,64 with a standard deviation of 0.11. We can expect that the ability of the SOPAFP method to study accurately the polarimetric properties of speckle fields at such intimate scale with the possibility to check the validity of the results, provide a better fundamental understanding of such fields, including depolarization and enpolarization effects [14] on the spatial variation of the SOP. On a more practical point of view, this new method could be used to optimize all the currently available optical techniques that use the strong characterization potential of speckle fields.

#218866 - $15.00 USD Received 28 Jul 2014; revised 29 Aug 2014; accepted 29 Aug 2014; published 25 Sep 2014

Acknowledgments

About the financial support of this work, we would like to thank the region Midi-Pyrénée for the APRTCN project and the French National Research Agency for the TRAMEL project.

#218866 - $15.00 USD Received 28 Jul 2014; revised 29 Aug 2014; accepted 29 Aug 2014; published 25 Sep 2014